

The Delphi Pixel Detector, running experience and performance

Natale Demaria^a on behalf of the Delphi Pixel Group

CERN, Geneva, Switzerland;
CPPM, Université Aix de Marseille II, Marseille, France;
IEK- Universität Karlsruhe, Karlsruhe, Germany;
Università di Milano and INFN, Milano, Italy;
LPNHE, IN2P3-CNRS, Universités Paris VI et VII, France;
Charles University, Praha, Czech Republic;
Collège de France, LPC, IN2P3-CNRS, Paris, France;
Wuppertal Universität, Wuppertal, Germany;
ISN, Grenoble, France.

^a CERN, CH-1211, Geneva23, Switzerland

The DELPHI Silicon Tracker has been optimised to satisfy the requirements of the LEP2 programme. It is made of a barrel part made by microstrip silicon detectors, upgraded from the old Vertex Detector, and the Very Forward Tracker (VFT) in the endcaps, composed on each side by two layers of pixel detectors and two layers of ministrip detectors. The use of pixels is crucial to allow stand alone pattern recognition thanks to the unambiguous three-dimensional determination of the track hit and the high efficiency. This dramatically improves the forward tracking in terms of efficiency and quality in the angular region between 25° and 10° w.r.t. the beam axis.

The Pixel Detector comprises 1.2 million pixels of $330 \times 330 \mu\text{m}^2$ size with 152 multi chip modules. It was partially installed in 1996, was completed in 1997 and it has collected data for two years. Module efficiency above 96 % and noise level below one part per million have been achieved.

A description of the detector is given and the running experience is reported. Results obtained are presented and the contributions to the forward tracking are shown.

1. Introduction and Motivations

The Delphi Silicon Tracker[1] is designed in order to satisfy the requirements posed by the physics programme at LEP2. The design takes into account the need for good hermeticity, giving emphasis to a good coverage of the tracking in the forward region[2], particularly important at LEP2 because of the following features of the processes studied or searched for:

- four fermion processes, important for both standard and non standard physics are relatively frequent, hence a larger angular coverage in polar angle is required compared to Z^0 physics.
- processes with the largest cross section, such as $e^+e^- \rightarrow q\bar{q}\gamma$ or $e^+e^- \rightarrow \gamma\gamma$ produce particles predominantly in the forward di-

rection

The tracking below 25° for the Z^0 programme is provided by the forward wire chambers FCA and FCB[3] located far away from the interaction point, at $Z = 155$ cm and $Z = 275$ cm respectively and after more than one radiation length of material. The presence of γ s confuses the tracking of forward wire chambers because of the high probability to shower before or between them, therefore creating a region with high density of hits belonging to the shower. In hadronic jets, where all π^0 particles decays into two γ s, this causes both a low tracking efficiency and several unassociated neutral clusters in the electromagnetic calorimeters. To improve this situation for LEP2 it has been necessary to build a tracking detector close to the interaction point and able to provide stand alone pattern recognition.

The Silicon Tracker is the upgrade of the Delphi Vertex Detector[4]. The acceptance of the barrel part is extended from 40° to 25° in polar angle and it is made of microstrip silicon detectors, two layers out of three measuring both coordinates. In the barrel region the pattern recognition relies mainly on the tracking detectors, the most important of which is the TPC. In the forward region strip detectors alone are not capable of providing stand alone pattern recognition, due to the enormous amount of spurious combinations of hits and ghosts tracks that would arise.

For this reason pixel[5] detectors are adopted, in order to provide unambiguous three dimensional points with which to build tracks elements with high purity and efficiency. Naively, it could seem an ideal solution to use several layers of pixels detectors, but studies show that a combination of two internal layers of pixel detectors and two external layers of ministrip detectors is an adequate choice, and furthermore reduces substantially the cost of the project. The choice of the cells dimensions is determined by the fact that momentum resolution is limited anyway by Coulomb scattering such that a hit resolution of $100 \mu\text{m}$ is sufficient.

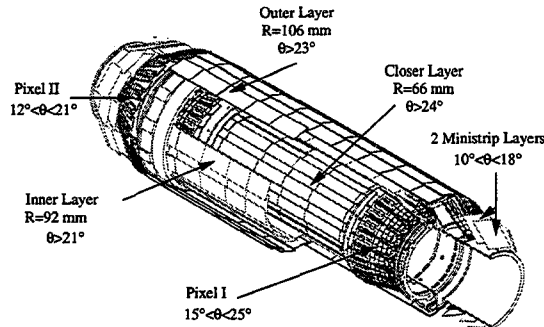


Figure 1. Layout of the DELPHI Silicon Tracker

The endcaps of the Silicon Tracker are therefore composed of two layers of pixel detectors, with cells of $330 \times 330 \mu\text{m}^2$, and two layers of back-to-back ministrip detectors with readout pitch of $200 \mu\text{m}$ and one intermediate strip. The endcaps cover the angular region $10^\circ - 26^\circ$ and $154^\circ - 170^\circ$ and they are called Very Forward Tracker (VFT in the following). The Silicon Tracker is illustrated in figure 1.

The design of the VFT has to satisfy the mechanical requirements on the Silicon Tracker. The space constraints are provided by the inner radius of the Inner Detector and the radius of the beam pipe and the total length of the detector must be limited to 1050 mm, in order to be able to install the structure inside DELPHI. The mechanical design must also be sufficiently rigid to support all components and suffer as little stress as possible from the varying deformations of the different components with changes of temperature, humidity, etc. At the same time, the extra support material must be kept to a minimum, so as to maintain the previous performance for the $R\phi$ impact parameter resolution in the barrel section. Figure 2 shows diagrammatically a cross section

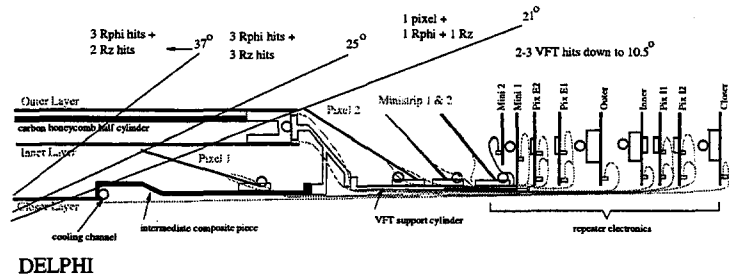


Figure 2. Cross section of one quadrant of the Silicon Tracker for $z>10\text{cm}$

of the modules and supports for one quadrant of the detector. It is evident how little is the space available for the internal pixel layer that is accommodated inside the Barrel part and this determines an angle of inclination of only 12° w.r.t. the beam axis.

The mechanical support consists of light aluminium endrings joined by carbon-honeycomb half cylinders. The internal pixel layer is accommodated on a composite piece that connect the endring of the Barrel closer layer with the Barrel endrings. The thermal expansion coefficients between the components are matched to reduce mechanical stress.

An adaptor piece connects the barrel to the forward cylinders. The forward cylinders support the external pixel layer and the two ministrip layers, and also serve to route the kapton cables towards the repeater electronic boards.

The resulting structure maintains the amount of material in the barrel at a similar level to the 1994-95 Vertex Detector, and moves forward material to significantly lower polar angles than previously. A photograph of part of the detector can be seen in figure 3.



Figure 3. Photograph of part of the detector showing from left to right R_z detectors of the Outer layer with their hybrids, the second pixel layer, two ministrip layers and part of the repeater electronics.

2. Experimental conditions

Before going to describe the Pixel Detector, it is important to define the experimental conditions in which it is working. They are mild compared to those of a hadronic machine.

The time between two crossovers (BCO) at LEP, when running with 4 bunches is $22 \mu\text{sec}$, giving the detector no problem to have the data ready to be read out every BCO. The Pixel Detector does not contribute to the trigger and it is read out every second level trigger. The trigger rates are 600 Hz for level one and less than 5 Hz for the second level: readout times are not very stringent.

The radiation level in the detectors is also very mild. It is constituted by off momentum electrons, often showering just in the material before the detector and by synchrotron radiation. The irradiation of the Pixels is estimated to be at the level of $< 1 \text{ kRad per year}$.

3. Detector description

3.1. Sensor

A sensor module consist of a pixel silicon detector with p^+ diodes on a n substrate $300 \mu\text{m}$ thick, with high resistivity of $5-10 \text{ k}\Omega\text{cm}$ determining a depletion voltage of 40-60 Volts. It consists of 10 areas each with 24×24 pixel cells and 6 with 18×24 pixel cells, each area corresponding to a readout chip. The pixel cell has a dimension of $330 \times 330 \mu\text{m}^2$ but cells in the boundaries between different areas have dimensions doubled in order to avoid dead regions due to readout chips being few hundred μm apart one another. A picture of a sensor is in figure 4 where from the shape it is clear why they are called raquettes. Overall dimensions are length of about 7 cm and width of 2 cm. The Delphi pixels adopt a hybrid solution therefore each sensor is bump bonded to 16 electronic chips. The area available for the bonding on the pixel cell has a diameter of $140 \mu\text{m}$.

The digital signal for the electronic chips are routed on the sensor, where a bus is integrated using double metal techniques. A guard ring surround the sensitive area. Supply lines to the chips do not go directly through the integrated bus be-

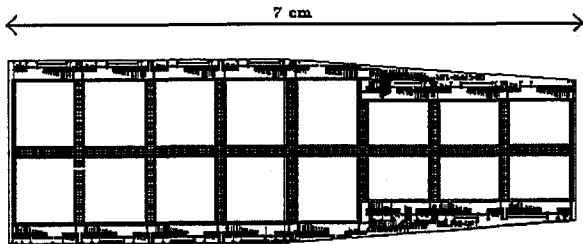


Figure 4. *Pixel sensor*

cause of voltage drop on the resistive lines. A kapton foil is glued instead on top of the chips and distributes the supply lines close to the single chips; then via bonding wire they are connected to the integrated bus and reach the chips.

One raquette has in total 8064 pixel cells. The supplier of the sensor is CSEM¹, the design was done at CPPM².

3.2. Readout chip

The readout chip is called SP8³[6]. It is a VLSI chip in 3 μm technology and provides preamplification, shaping, discrimination and binary readout of cells with signal, using a 2D sparse data scan[7] and each signalled cell is readout in 200 ns. On two cells per chip, a *p*-well underneath the input pad defines a 30 fF calibration capacitance. The power consumption of the chip is of 40 μW per cell.

The threshold is adjustable between 5 to 20 ke $^-$, with 1.2 ke $^-$ RMS. From test beam data it has been proven that in the configuration of Delphi Pixel detectors, for a threshold up to 10 ke $^-$, an efficiency of 99 % is obtained.

The interconnection via the integrated bus is highly demanding in terms of failure rate of the interconnection technique. The connection be-

tween the bus lines and the corresponding pad on the chip is achieved by the same bump-bonding technique used for the pixel interconnection. The IBM C4 (Controlled Collapse Chip Connection) bump bonding process⁴ was used with 100 μm bond diameter on a 140 μm diameter bonding area. A $(2.4 \pm 0.2) \times 10^{-4}$ failure rate was achieved, that determines 80% raquette efficiency due to bump bonding.

The SP8 is designed for a milder environment than LHC so it works stably for occupancy < 20% and it has a radiation tolerance of 10 kRad.

3.3. Assembly of a Raquette

The assembly of the raquette module is done in several steps:

- 16 SP8 chips are bump bonded to the detector;
- the ceramic providing the mechanical support of the raquette is aligned and glued;
- the 4 layer flat kapton⁵ is glued on top of the SP8 chips;
- long kapton⁶, providing the connection to the repeater electronics, is glued;
- wire bonding is done to connect: long kapton to flat kapton lines and then to the bus integrated on the detector; flat kapton to the supply lines on the detector.

The assembly of a pixel raquette is illustrated in figure 5. The complete raquette module determine less than 1% X_0 of material budget.

The yield of production at the several steps of the assembly is: 77% after dicing and bump-bonding; 68% for a full functioning of the readout of all 16 SP8 after the connection to the raquette and 85 % for the remaining phase of the assembly, including mounting on crowns and finally on the Silicon Tracker mechanical support. Taking into account also the 82% rate for accepting the sensor before considering the assembly, the total yield rate become of 36%.

¹CSEM, Rue de la Maladière 41, CH 2007, Neuchatel, Switzerland

²CPPM , Centre de Physique de Particules de Marseille

³Designed by College de France, Paris and CPPM; Made by FASELEC 3 μm technology, Phyllips (Taiwan).

⁴Metallisation done by IBM, Corbeil (France); flip-chip by IBM Montpellier (France)

⁵Design of CPPM; Made by TELEPH

⁶same reference of the flat kapton

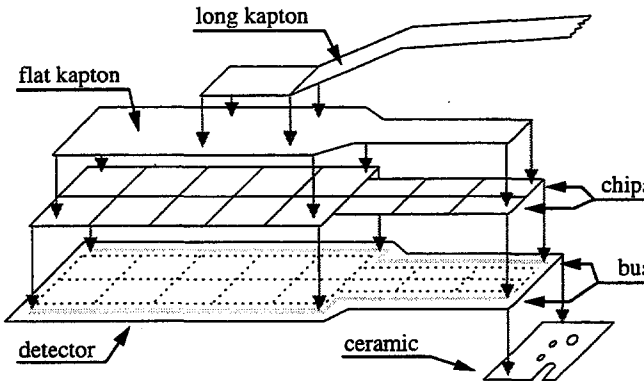


Figure 5. Assembly of a pixel raquette

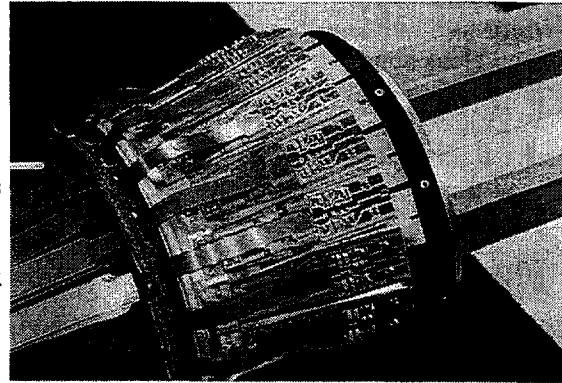


Figure 6. Photograph of an assembled inner layer pixel crown.

3.4. Crown

The pixels raquettes are mounted onto semicircular aluminium supports, with inclinations with respect to the z axis of 12° and 32° for the pixel and are arranged in groups of 19 forming a pixel crown. The raquettes are connected to the repeater boards with the long kapton cables, with two repeater boards per crown. A photograph of a pixel crown is shown in figure 6. There are 8 crowns, for a total of 152 raquettes and 1.2 millions pixels for a sensitive area of 0.2 m^2 .

Overlap between adjacent raquettes is provided in order to allow internal alignment: for the inner and outer pixel layers the overlap corresponds to 37% and 12%.

3.5. Readout system

The readout system[7] consists of a crate processor housed in a fastbus crate controlling 4 fastbus modules (PIxel Read-Out Modules PIROM) and reading them sequentially. Each PIROM contains 4 PIxel Read-Out Unit (PIROU) based on a micro-controller Motorola 68332, connected each one to one repeater board, and all PIROU are read in parallel. Each PIROU controls a group of 10 or 9 raquettes connected to the repeater, addressing and reading sequentially each chip of each raquettes. The readout scheme al-

lows the skipping of malfunctioning/not responding chips. A mask of noisy pixels can be loaded on the PIROU in order to suppress them: this is particularly important in order to keep the size of the pixel data low avoiding unnecessary information.

3.6. Slow Control system

Stable and safe operation is a critical issue for running the Pixel Detector. There is an automated response to changes in the data taking conditions or possible misbehaviours of the detector, running within the framework of the general DELPHI slow controls system.

The slow control frontend-computer for the Pixel[9] is based on a 68340 processor running OS9 and the main components are a commercially available SY527 CAEN and a home made DAC-system.

The CAEN⁷ controller supervises power supplies and depletion voltages for a total of 88 channels, distributed at the level of repeater or crown. The threshold settings is done at the level of single raquettes in order to optimise the working point of each one in terms of efficiency and noise per-

⁷Costruzioni Apparecchiature Elettroniche Nucleari S.p.A., Via Vetraia, 11, I-55049 Viareggio, Italy

formance. It is controlled by the DAC system

A procedure was developed to detect and react to an anomalous number of hit pixels, associated to either a high background or to a misbehaving chip. It is necessary to protect the detector against accidental very high occupancies because the power consumption of a cell connected to a hit pixel increases by a factor of about 10. If the required power exceeds the supply characteristics the detector may then trip off, leading to a jump in temperature of around 12°C , affecting badly the detector stability. A typical situation where this can arise is during the LEP injection, when the occupancy can be up to more than 2 orders of magnitude greater than nominal. When the occupancies are abnormally high the crate processor supervising the data acquisition notifies the slow control system, which raises the thresholds [9]. In addition, for the special period of LEP injection when the backgrounds are expected to be high, the discriminator thresholds are always automatically raised.

4. Performance

4.1. Noise level

The level of systematically noisy pixels is around 0.3%. Most of the noisy pixels are removed by masking in the crate processor, and the remaining ones, defined as those which respond to more than 1% of triggers, are flagged and removed off-line.

After the removal of noisy pixels, the hits which remain originate from particles traversing the detector and from random noise. The number of pixel hits is shown in figure 7 for three classes of events. Hadronic events, where some tracks pass through the forward region, have a mean number of pixel hits of about 4.5. Background events, which are triggered events with no tracks pointing to the primary vertex, include beam gas interactions at low angle and off-momentum electrons than might have showered before the Pixel, and result in a tail extending to very large numbers of hits. Such events become more prevalent at higher energies.

A class of events was also selected with just two charged tracks reconstructed in the barrel. These

events should produce no physics background in the forward region, and the mean number of pixel hits places an upper estimate on the random noise of 0.5 ppm.

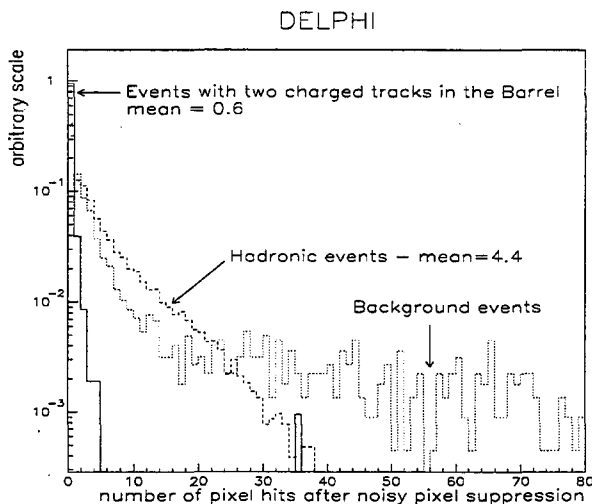


Figure 7. *Mean number of pixels per event for hadronic events, background events, and events with two charged tracks only in the barrel. The data are taken from the 1997 Z^0 running period. The normalisation is arbitrary.*

4.2. Alignment

The alignment of the full Silicon Tracker consists of a survey stage and an alignment using tracks.

The pixel detectors are surveyed in two steps. After the chips are bump-bonded and the ceramic support is glued to the detector, the two-dimensional position of the external detector corners and the ceramic are determined with a microscope with respect to pads close to the detector corners.

These pads have a well known position on the detector mask and define the position of the pixel

array. They are chosen as a reference as they remain visible during the assembly. The kapton cables are then attached and the tested module mounted on the support. Its position, given by the location of the two corners plus the measurement of the module's plane, is related to that of three spheres mounted on the support. After all modules are mounted, the VFT crowns are joined to the barrel support and the positions of the spheres with respect to the barrel are measured.

Being the survey made before the installation inside DELPHI, the survey gives no information on the relative position of the two half-shells. Also the geometry of either half-shell after installation might slightly differ from the results of the survey, due to possible deformations of the mechanical structure. The survey is therefore the starting point for the alignment done using tracks.

The VFT alignment procedure uses track elements already reconstructed with the use of the other tracking detectors. The procedure optimises the VFT module positions by minimising the χ^2 of tracks refitted over all track elements. The weight of a track in the fit depends on the polar angle and the combination of tracking detectors contributing to the track. In addition, the intrinsic VFT resolution and the constraints from overlapping modules are exploited. The global parameters at the level of each quadrant are determined first, then the individual plaquette parameters are fitted, allowing 6 degrees of freedom per plaquette. The overlap between the first pixel layer and the Barrel Inner layer at $20^\circ < \theta < 25^\circ$ provides a good link between the Barrel and the VFT global alignment.

4.3. Efficiency

The efficiency of the pixels was studied using tracks which pass through a region where neighbouring plaquettes overlap and have at least one hit in a silicon layer other than the one being studied. If a track registers a hit in one plaquette, a second hit is searched for around a 3σ window in the neighbouring plaquette. Figure 8a shows the average efficiency measured in each pixel crown using this technique. The average efficiency excluding bad plaquettes was 96.6%.

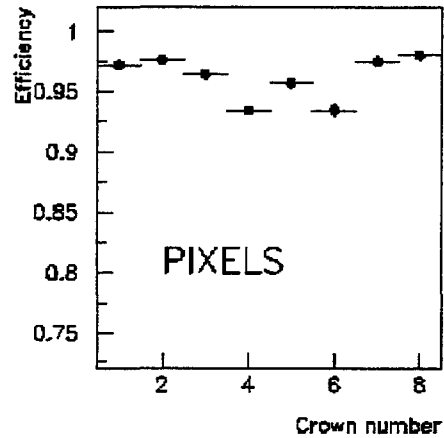


Figure 8. Efficiency for the pixel crowns as measured in the 1997 data using tracks (see text). The average quoted efficiencies do not take into account dead modules.

4.4. Resolution

For the pixels, the expected resolution depends on the cluster size, which is a function of the track incidence angle. Tracks from the primary vertex traverse the first and second pixel layer at incidence angles ψ in the polar direction of 57.5° and 40.5° respectively. The incidence angle in the $R\phi$ direction is close to 90° . The majority of produced clusters are either single hits or double pixel hits split in the polar direction. Neglecting charge diffusion effects, the angular dependence of the single pixel hit rate is given to first order by the following equation:

$$N = (1 - \frac{d}{\Delta}); \quad d = w \times \tan\psi - \frac{t}{c} \times w \times \sin\psi \quad (1)$$

where w is the thickness of the depletion layer, Δ is the pixel pitch, c is the charge deposited by a minimum ionising particle and the parameter t is given by the detector threshold (about 10ke^- is used). Knowing this rate, a simple geometrical consideration of ionisation charge sharing in the pixel sensitive volume leads to the following

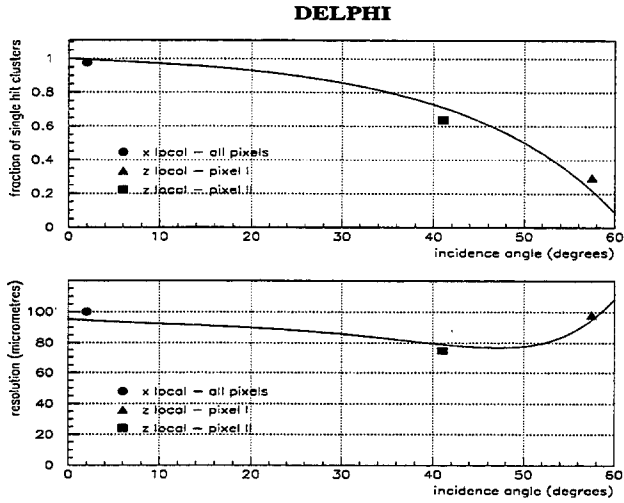


Figure 9. Resolution expected in the pixels as a function of track incidence angle (solid line) shown together with the values measured in the data.

expression for the expected detector resolution:

$$\sigma^2(\psi) = \frac{1}{12} \frac{(d^3 + (\Delta - d)^3)}{\Delta} + \left(\frac{\kappa}{c} \times w \times \sin\psi\right)^2 \quad (2)$$

Here κ is a parameter describing the effect of charge fluctuations (about 5ke^- is used), and the other symbols are the same as in equation 1.

The expected distributions are displayed in figure 9 as a function of ψ . The resolutions in the data are measured in the detector plane for the z_{local} (polar) direction and the x_{local} ($R\phi$) direction. The values extracted are overlaid on the prediction. For the x_{local} points the incidence angle is the same for the pixel I and pixel II layers, and these points are shown together. The measured points are seen to be very close to those predicted by the simple model.

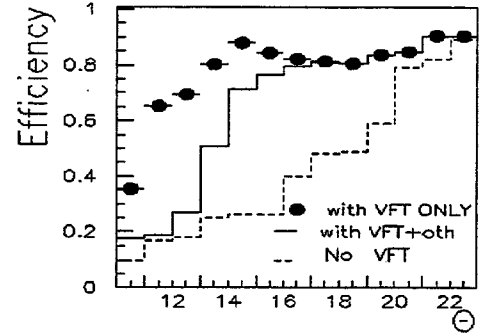
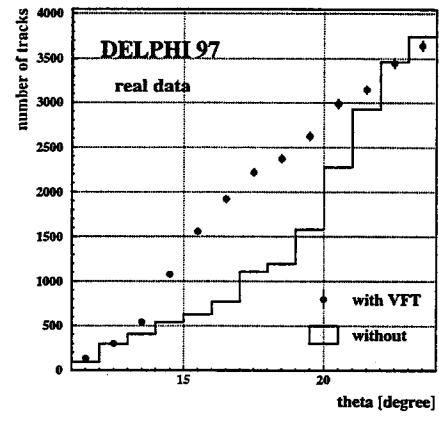


Figure 10. Improvement on the forward tracking thanks to the Pixel Detector in the VFT

5. Improvement in Forward Tracking and Hermeticity

Improvements of the forward tracking using the VFT data have been studied both at Montecarlo level, using the full reconstruction software of Delphi, and on real data. The performance of the tracking both excluding and including the VFT data has been compared.

In the upper part of figure 10 is the number of tracks versus polar angle for real data collected in 1997, when including or not the VFT in the tracking. To measure an absolute tracking efficiency on real data is difficult since there is no redundancy in the forward tracking to do so. Therefore in the lower part of figure 10 is the tracking efficiency as measured on MC, with and without VFT.

Comparisons on data/MC of the ratio of number of tracks obtained with and without VFT give a good agreement giving confidence on values found by the MC studies.

When quoting *with VFT* is meant that the VFT is contributing to form a track together with another tracking detector (mainly FCA and FCB).

It was mentioned in the beginning of the paper that VFT provides standalone pattern recognition, and in certain cases a good VFT track might not find a clear association to the other tracking detectors. These tracks, called VFT only tracks, reach a high purity, greater than 95% when including hits from 3 layers and therefore they improve substantially the tracking hermeticity down to about 10°. In figure 10 is shown the tracking efficiency obtained when this category is added. The VFT only tracks have a poor momentum resolution but the direction of the track at the VFT is measured with 1-2 mrad precision. The use of the VFT only tracks is exemplified in picture 11 where a real event having two high energy deposit in the electromagnetic calorimeters but no tracks associated to them is shown. Including VFT only tracks, two tracks are visible, allowing to determine that the event is a Bhabha in the forward direction.

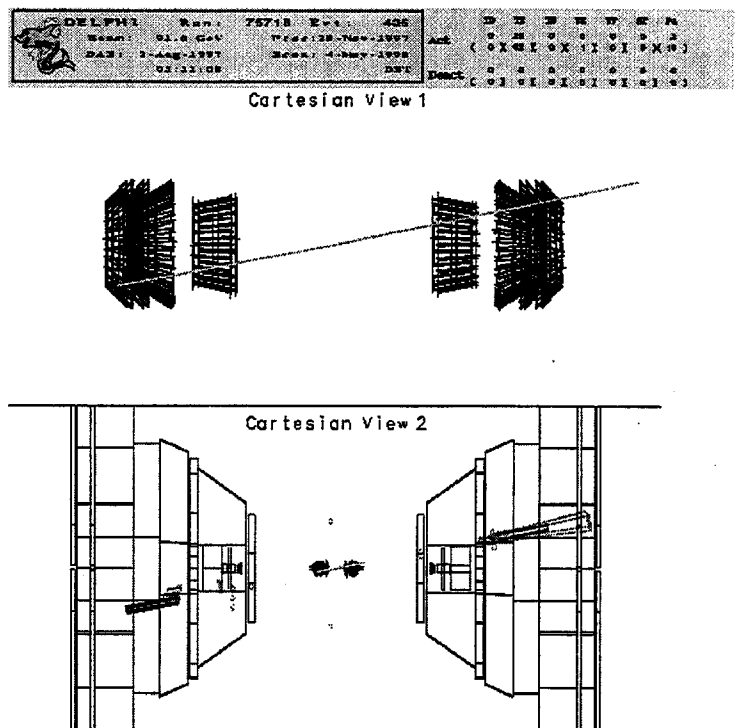


Figure 11. *Bhabha event with tracking provided by the VFT*

6. Conclusions

The Delphi Pixel Detector was commissioned on 1996 and then completed on 1997. Stable running performance have been obtained and the design performance has been achieved: random noise level of 0.5 ppm and single plane efficiency of 96% with a hit resolution of 80-100 μm .

This allows Delphi Silicon Tracker to satisfy the request imposed by the LEP2 programme. The VFT has been fully integrated in the tracking of Delphi and this has dramatically improved the tracking efficiency in the forward region.

Acknowledgements

This paper is presenting the results achieved thanks to the common effort of the entire Delphi Pixel group. I want to thank all my colleagues for the brilliant work done and for having supported me for this presentation.

REFERENCES

1. V.Chabaud et al., *The DELPHI Silicon Tracker at LEP2*, Accepted by Nucl. Instr. and Meth. **A** (1998).
2. The DELPHI Collaboration, *Proposal for the upgrade of DELPHI in the Forward Region*, CERN/LEPC/92-13/P2 Add2, 16th October 1992.
3. P. Abreu et al., (DELPHI Collaboration), *Performance of the DELPHI Detector*, Nucl. Instr. and Meth. **A378** (1996) 57.
4. V.Chabaud et al., *The DELPHI silicon strip microvertex detector with double-sided read-out*, Nucl. Instr. and Meth. **A368** (1996) 314.
5. D.Sauvage et al., *A Pixel Detector for the '95 Upgrade of the DELPHI Micro Vertex Detector*, CPPM - 95-05 and Proceedings of the fourth International Workshop on Vertex Detectors, June 1995, Ein Gedi Resort, Dead Sea, Israel, p. 53.
K.H.Becks et al., *Progress in the construction of the DELPHI pixel detector*, Nucl. Instr. and Meth. **A395** (1997) 398-403
K.H.Becks et al., *The DELPHI pixels*, Nucl. Instr. and Meth. **A386** (1997) 11.
6. M. Cohen-Solal and J.C. Clemens, *Electronics for pixel detectors*, Nucl. Instr. and Meth. **A380** (1996) 335.
7. J.J. Jaeger et al., *A sparse data scan circuit for pixel detector readout*, IEEE Trans. Nucl. Sc. 41, no.3 (1994), 632-636.
8. C. Aubret, J.M. Brunet, B. Courty, L. Guglielmi, G. Tristram, J.P. Turlot, *DELPHI Pixel Detector Readout*, Collège de France, Paris, September 13, 1996, available via WWW:
http://cdfinfo.in2p3.fr/Experiences/Delphi/VFT/vft.html
9. S. Kersten, *Slow Control for the DELPHI Pixel Detector*, University of Wuppertal, May 9, 1997, available via WWW:
http://www.uni-wuppertal.de/FB8/groups/Drees/detlab/vft_slowctrl.html